14th International Symposium on Turbulence and Shear Flow Phenomena (TSFP14)
Heidelberg, Germany, July 28–31, 2026

ESTIMATION OF POWER SPECTRA AND CROSS-SPECTRA FOR ALL THREE VELOCITY COMPONENTS FROM PIV MEASUREMENT DATA

Lionel Larchevêque
Aix-Marseille Univ
IUSTI, CNRS
Marseille, France
lionel.larcheveque@univ-amu.fr

Deepak Prem Ramaswamy
Institute of Fluid Mechanics and Aerodynamics
Universität der Bundeswehr München
Neubiberg, Germany
deepak.ramaswamy@unibw.de

Anne-Marie Schreyer
Department 03 - Mechanical, Automotive and Aeronautical Engineering
Hochschule München University of Applied Sciences
Munich, Germany
anne-marie.schreyer@hm.edu

ABSTRACT

We present a method to estimate power spectra and cross-spectra from all three velocity components acquired at discrete time delays. Building on a convection-based reconstruction approach, temporal cross-correlations are transformed into a Blackman-Tukey estimate of cross-spectral density, which can further be used for spectral proper orthogonal decomposition (SPOD), enabling modal analysis of non-time-resolved measurements. Validation of the approach on large-eddy simulations (LESs) of a Mach 2.52 shock-wave / boundary-layer interaction demonstrates good recovery of power spectra, coherence and phase spectra. Application of the Blackman-Tukey direct SPOD to stereo-dual-PIV measurements shows good agreement with the LES results, demonstrating the potential of the method for extracting three-dimensional spectral dynamics and coherent structures in high-speed turbulent flows.

CONTEXT AND MOTIVATION

Supersonic turbulent flows of Reynolds numbers typically encountered in wind-tunnel experiments have characteristic time scales of $\mathcal{O}(100\,\text{kHz})$ for the most energetic eddies of the boundary layers. This frequency implies that a time-resolved measurement device should have sampling rates of several hundred kHz to prevent aliasing when performing spectral analysis. Multipoint velocity measurement techniques such as Particle Image Velocimetry (PIV) struggle to reach this requirement, which is achieved at the expense of the spatial resolution and signal duration even for more advanced setups.

One alternative to recover temporal information from PIV measurements is the dual-PIV approach, as e.g. described in Schreyer *et al.* (2015). In dual-PIV systems, two pairs of high-resolution images are sampled at a low rate, but with a delay between the two pairs that can be made arbitrarily small. Therefore, cross-correlations between the two velocity fields can be computed for this time delay. By carrying out measurements with multiple delay times, it is possible to obtain discretizations of the temporal evolution of the cross-correlations.

However, acquiring data for a single time delay requires an equivalently high experimental effort as for classical PIV measurements. The number of achievable time delays is therefore limited. Consequently, a straight Fourier transform of the sampled cross-correlation function yields spectral estimates with very poor frequency resolution.

Schreyer *et al.* (2016) and Jiang *et al.* (2017) addressed this problem by taking advantage of the high spatial resolution of the PIV data to perform physically informed temporal interpolations of the cross-correlations. The method efficiently reconstructed estimates of the power spectrum of the streamwise velocity component, accurate up to over 100 kHz across the entire flow field.

In the present work, we extend the estimation of power spectra to all three velocity components, as well as to cross-spectra. We use this interpolation-based methodology to extend the spectral analysis of a joint experimental – numerical database of a $M_\infty = 2.52$ shock–wave/boundary–layer interaction obtained from the compression–expansion corner setup described in Larchevêque *et al.* (2023).

We use the available stereo–dual PIV measurements to extend the method of Jiang *et al.* (2017) to estimate power spectra of all three velocity components, and also to cross-spectra between any locations and velocity components in the flow field. Such two-point spectral data allow us to analyze couplings between the various regions of the flow. They also formally enable computations of TKE–based Spectral Proper Orthogonal Decompositions of (part of) the flowfield, thus allowing us to complement our earlier analysis of this data base.

The development strategy relies on a validation of the cross–spectral reconstruction method using the LES database from which the true cross-spectra can also be obtained. It will take advantage of the long duration of the simulations to achieve reasonably converged spectral estimates. Once validated, the method is applied to the experimental database.

TEST DATABASES

The large-eddy simulations (LES) were performed for a $+24^\circ$ compression/-24° expansion interaction at $M_\infty = 2.52$ using the FLU3M solver with second-order spatial and temporal accuracy. The simulations covered about 90 characteristic low-frequency cycles of the separation bubble breathing motion, providing good statistical convergence. The LESs have previously been validated against PIV and Schlieren measurements under similar conditions, showing good agreement in terms of mean velocity profiles, POD mode shapes, and limited spectral data obtained from high-speed Schlieren image sequences. Further details of the numerical methodology and validation are provided by Larchevêque *et al.* (2023).

Additional stereo-dual-PIV measurements were conducted for the same 24° compression–expansion corner configuration under similar flow conditions at the Institute of Aerodynamics, RWTH Aachen University. The measurement system comprised four FlowSense EO 11M CCD cameras and two Litron lasers, configured according to Ramaswamy *et al.* (2023). Measurements were acquired at 6 Hz for selected system time separations. Optical color filters were used for image separation and vector processing was performed in Dantec DynamicStudio 7.0 using a final interrogation window of 32 px × 32 px with 75% overlap.

Between 550 – 700 double PIV image pairs have been sampled for each of the 9 discrete time delays $\tau_{i=0,\ldots,8} = [0,5,10,50,100,200,300,400,500]\ \mu$s between the two subsystems. The time delays were selected based on the tests presented in Jiang *et al.* (2017), which were related to a shock-boundary layer interaction with fairly similar time and space scales as the present one.

TWO-POINT CROSS-SPECTRAL DENSITY

Method

Assuming that dual-PIV measurements are available for a small number n of time delays $\tau_i, i = 1,\ldots,N$, the cross-correlation function for velocity components u_j and u_k between reference locations x_1 and $_2$, defined by:

$$R_{\mathrm{u_j u_k}}(\mathbf{x_1},\mathbf{x_2},\tau) = \left\langle u_j(\mathbf{x_1},t)\, u_k(\mathbf{x_2},t-\tau)\right\rangle - \left\langle u_j(\mathbf{x_1},t)\right\rangle \left\langle u_k(\mathbf{x_2},t-\tau)\right\rangle \quad (1)$$

as well as the cross-correlation coefficient $r_{\mathrm{u_j u_k}}(\mathbf{x_1},\mathbf{x_2},\tau)$ can be computed for both positive and negative time delays $\pm\tau_i$ using the time-average operator $\langle\cdot\rangle$.

The basic idea of the method described in Jiang *et al.* (2017) is to take advantage of the full cross-correlation information in space made available from the dual-PIV measurements by assuming a convection–dominated flow. The high resolution in space is used to compensate for the restricted discretization in time by considering the convected frame of reference to interpolate the correlation function between consecutive known values at τ_i and τ_{i+1}. This is conceptually similar to the Taylor hypothesis, but the convection assumption is invoked over short time intervals $[\tau_i, \tau_{i+1}]$.

The displacement of the velocity component u_j (respectively u_k) at location x_1 (respectively x_2) associated with convection is estimated from dual-PIV data by searching the separation distance $\Delta^{u_j}_{\mathbf{x_1}}$ (respectively $\Delta^{u_k}_{\mathbf{x_2}}$) for which the cross-correlation coefficients are maximum for every τ_i. Such values of the cross-correlation coefficient are formally similar to those of the Lagrangian autocorrelation coefficient $r^L_{u_j}(\mathbf{x_1},\tau)$ (respectively $r^L u_k(\mathbf{x_2},\tau)$). The displacement for any given τ is then estimated from these data using a smoothed piecewise linear interpolation, as described in Jiang *et al.* (2017).

By assuming a convective behavior for $\tau \in [\tau_i, \tau_{i+1}]$, the cross-correlation at time τ can be estimated from the known,

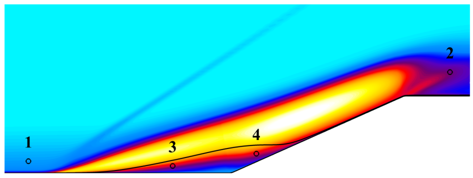

Figure 1. Map of turbulent kinetic energy of the present shock–wave/boundary layer interaction with superimposed locations of the test sensors.

space–shifted cross-correlations at times τ_i and τ_{i+1} as:

$$r_{\mathrm{u_j u_k}}(\mathbf{x_1},\mathbf{x_2},\tau) \simeq \begin{cases} r_{\mathrm{u_j u_k}}(\mathbf{x_1},\mathbf{x_2}+\Delta\mathbf{x_2}^{u_k}(\tau-\tau_i),\tau_i) \\ r_{\mathrm{u_j u_k}}(\mathbf{x_1},\mathbf{x_2}+\Delta\mathbf{x_2}^{u_k}(\tau-\tau_{i+1}),\tau_{i+1}) \end{cases} \quad (2)$$

where $\Delta\mathbf{x_2}^{u_k}(\tau-\tau_i)$ and $\Delta\mathbf{x_2}^{u_k}(\tau-\tau_{i+1})$ are estimated displacements of the reference frame for the variable u_k in the vicinity of the location x_2 with respect to time delays τ_i and τ_{i+1}.

The even parity of the autocorrelation function was used in Jiang *et al.* (2017) to obtain two additional estimates by considering the negative time delay $\tau \in [-\tau_{i+1}, \tau_i]$. The symmetry relation for the cross-correlation is slightly more complex and, using definition 1, reads $R_{\mathrm{u_j u_k}}(\mathbf{x_1},\mathbf{x_2},\tau) = R_{\mathrm{u_k u_j}}(\mathbf{x_2},\mathbf{x_1},-\tau)$. The additional estimates can thus be obtained by considering the displacements $\Delta\mathbf{x_1}^{u_j}(-\tau+\tau_{i+1})$ and $\Delta\mathbf{x_1}^{u_j}(-\tau+\tau_i)$ in the vicinity of x_1 for the variable u_j with respect to time delays $-\tau_{i+1}$ and $-\tau_i$:

$$r_{\mathrm{u_j u_k}}(\mathbf{x_1},\mathbf{x_2},\tau) \simeq \begin{cases} r_{\mathrm{u_k u_j}}(\mathbf{x_2},\mathbf{x_1}+\Delta\mathbf{x_1}^{u_j}(-\tau+\tau_{i+1}),-\tau_{i+1}) \\ r_{\mathrm{u_k u_j}}(\mathbf{x_2},\mathbf{x_1}+\Delta\mathbf{x_1}^{u_j}(-\tau+\tau_i),-\tau_i) \end{cases} \quad (3)$$

The four estimates obtained from Eqs. 2 and 3 are then weighted using a composite function relying on the relative time delays $\tau_{i+1}-\tau$ and $\tau-\tau_i$ as well as on the local values of the Lagrangian auto-correlation for u_j and u_k at times $\pm\tau_i$ and $\pm\tau_{i+1}$, as described in Jiang *et al.* (2017). The resulting upwind–biased scheme adapts to the local validity of the convection assumption in both the upstream and downstream directions.

Once the cross-correlation coefficients $r_{\mathrm{u_j u_k}}(\mathbf{x_1},\mathbf{x_2},\tau)$ have been reconstructed for any desired time delays $\tau \in [-\tau_N, \tau_N]$, a Blackman-Tukey estimate of the cross-spectral density $S_{\mathrm{u_j u_k}}(\mathbf{x_1},\mathbf{x_2},f)$ can be obtained by renormalizing them using the geometric mean of the respective variances and then Fourier-transforming them. The frequency resolution Δf of the estimate is set by the value of τ_N as $\Delta f = \mathscr{O}\left(\tau_N^{-1}\right)$, depending on the window, if any. The maximum frequency for which a reliable estimator can be obtained is, however, limited by the spatial aliasing associated with the spatial resolution of the measurement grid Δx and the convection velocity U_c.

Assessment of the LES database

Power- and cross-spectra involving the three velocity components obtained at 40 locations distributed throughout the compression-ramp interaction have been computed and analyzed. For the sake of conciseness, results are presented only for the four locations highlighted in Fig. 1, which are representative of the best/worst performances that the two reconstruction schemes under evaluation can achieve.

In the two evaluated schemes, the power spectra are either estimated using all the time delays available in

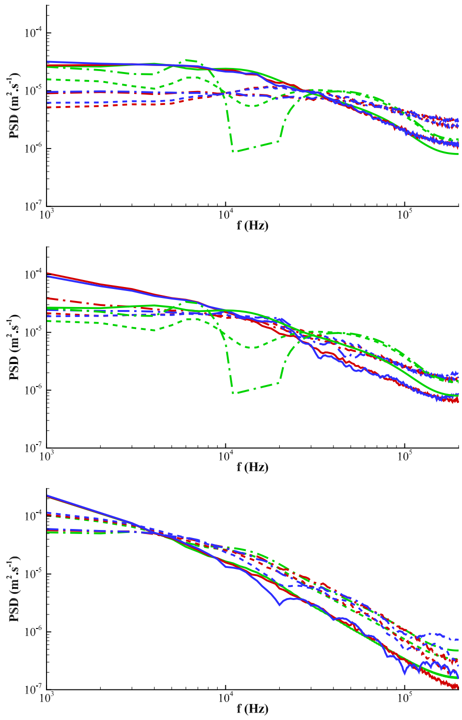

Figure 2. Power Spectral Densities of velocity components computed from the whole database (red) and from the available $\Delta\tau_i$ from interpolation based on the cross-correlation field (blue) and a natural spline (green). Streamwise (solid), wall–normal (dash-dot) and spanwise (dashed) components at locations 1 (left), 2 (center), and 3 (right) as indicated in Fig. 1.

the LES database ("exact" cross-correlation) or only the ones listed above ($\tau_{i=0,\ldots,8}$), supplemented with interpolations of the cross-correlation that rely either on the present cross correlation–based scheme or pure mathematical natural splines. The results are compared in Fig. 2. For locations 1 and 2, the spline interpolation results in oscillations for the v and w spectra that were not identified from the sole u spectra computed in Jiang *et al.* (2017). The main, moderate artifact found in spectra obtained from the present method lies in regions of high streamline curvature (sensor 3) for u, as already seen in Jiang *et al.* (2017).

Coherence and phase spectra between locations 1–2 and 3–4 are displayed in Fig. 3 for streamwise–streamwise and streamwise–wall normal components for the former (top and middle two plots, respectively), and streamwise–streamwise component for the latter (bottom two plots). Overall, the two interpolation schemes result in the same accuracy up to 10 kHz. Beyond that range, the present cross-correlation-based method gives superior results as far as the "exact" coherence is statistically significant. Note that the few overshoots seen for the present method in the 3–4 coherence spectrum (bottom pair of plots in Fig. 3) is a direct consequence of the normalization of the cross-spectrum by the locally, slightly underestimated power spectrum of u at location 3: the norm of the cross-spectrum does not suffer such artifacts.

EXTENSION TO SPECTRAL POD

Method

The standard way for performing SPOD is based on the snapshot method (Sirovich (1987)) reformulated within

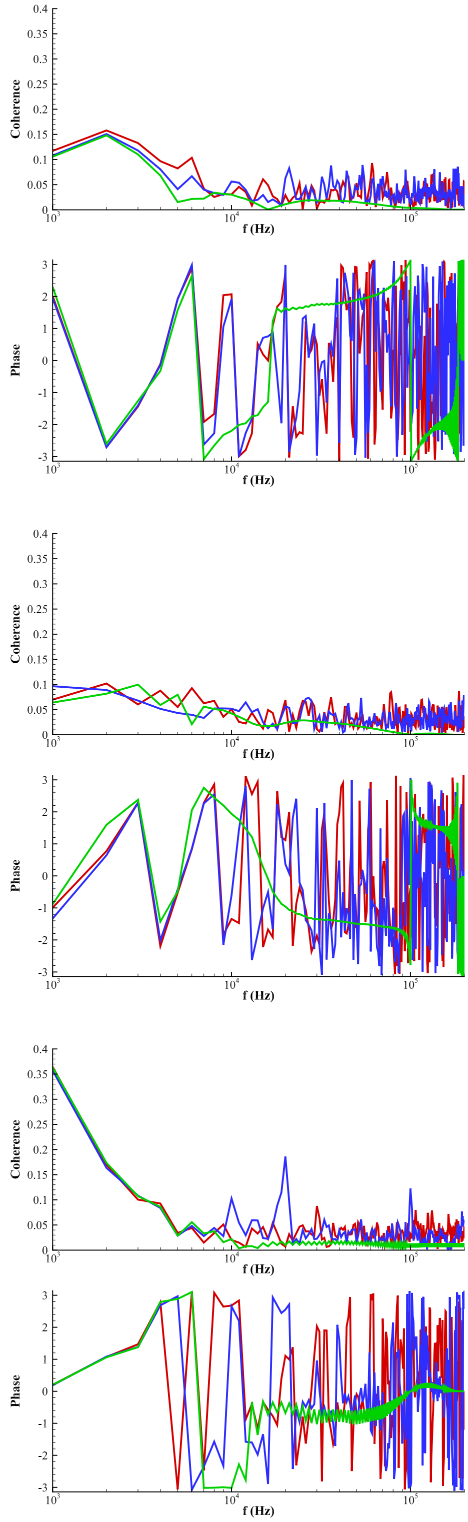

Figure 3. Coherence and phasespectra computed from the whole database (red) and the $\Delta\tau_i$ available from interpolation based on the cross-correlation field (blue) and the natural spline (green). Streamwise velocity components between locations 1 and 2 (top two subfigures), cross-streamwise–wall-normal components between locations 1 and 2 (middle plots), and streamwise velocity components between locations 3 and 4 (bottom pair of plots).

Welch's spectral estimate formalism, see for instance Schmidt & Colonius (2020). This approach (hereafter denoted by Welch-snapshot), though extremely computationally efficient, cannot be applied to the velocity fields measured with dual-PIV, as these are inherently not time-resolved. The alternative is to revert to the original POD approach proposed by Lumley (1967), known as the direct method, and to apply it to the cross-spectral matrix. This method is referred to as Blackman-Tukey Direct in the remaining part of this paper.

The main drawback of the Blackman-Tukey Direct method is that the computational and memory cost associated with the building of the SPOD matrix scales with the square of the number of points under consideration. As an illustration, the computation of a 10,000 points SPOD for 25 distinct frequencies with three velocity components from the present experimental database would require, using the Fortran-OpenMP code developed for that purpose, about 3 days on a 36-core workstation and 400 GB of memory. However, it is worth noting that the number of points can be significantly reduced by clustering them into regions of physical interest.

Since a large number of points need to be processed without the possibility of manually adjusting local parameters (such as the significance threshold for Lagrangian autocorrelation when determining trajectories, for example), we made the reconstruction algorithm described in the previous section more robust in two respects. Firstly, the weighting of the four estimates defined in Eqs. 2 and 3 now relies only on the Lagrangian correlation coefficients associated with them, to better discriminate between reliable and unreliable ones. Secondly, the spline-like spatial interpolation scheme used to reconstruct the displacement has been replaced with a Stineman (1980) interpolation to remove overshoots in cases of strong acceleration.

Assessment from the LES database

SPOD modes were computed for a single streamwise–wall normal plane, taking into account the three velocity components either over the whole duration of the LES (88,800 time samples encompassing about 90 cycles of the low–frequency breathing of the separated region) or over one seventh of it (12,000 samples). We used three different methods to extract the modes: standard Welch snapshot and Blackman-Tukey Direct with a) "exact" cross-correlation and b) interpolated cross-correlation from the set of sampled time delays $\tau_{i=0,\dots,8}$ listed previously. The methods were applied to a grid of 70×16 points distributed over a streamwise–wall-normal plane with the same streamwise extent as the field shown in Fig. 1.

The turbulent Kinetic Energy spectra integrated over this grid, global or for modes 1 and 10, are plotted in Fig. 4. As expected, the two methods using all time samples yield almost identical results. The spectra obtained using the reconstruction method stand out in two respects. Firstly, aliasing is observed above 150 kHz and secondly, peaks corresponding to harmonic frequencies of 10 kHz are found in the first two modes. The origin of these peaks can be traced back to spurious overshoot of the reconstructed cross-correlation in the vicinity of known time delays $\tau_i = 100$ to $500\ \mu s$ for regions where convection is not the dominant coherent process. Mostly, the head shock and its neighborhood are affected, with distinct characteristic time scales for the two processes.

The spatial modes displayed in Fig. 5 essentially tell the same story. When using the Blackman-Tukey method with the reconstructed cross-correlations, extra spurious modes are inserted, whose energy is concentrated near the head shock, as visible in the central column. When projecting the differences between the cross-spectral density estimates obtained from the Blackman-Tukey method applied to the "exact" and reconstructed cross-correlations (*i.e.* the spectral error of the reconstruction scheme) onto the SPOD modes, we found that the energy of these spurious modes essentially comes from this spectral error, as visible in the last line of Fig. 5.

Lastly, when we reduce the number of samples from which SPOD is computed, the energy content of the dominant modes is increased in the high frequency range because of a lower ability to discriminate between the physical fluctuations of lower spatial coherence and the increased statistical uncertainty of the spectrum estimates. Here too, the spectra obtained from the reconstructed intercorrelation stand out, as they are less susceptible to this effect. It can be postulated that the reconstruction algorithm, being inherently based on a coherent process, tends to reinforce the coherent component relative to the statistical uncertainty.

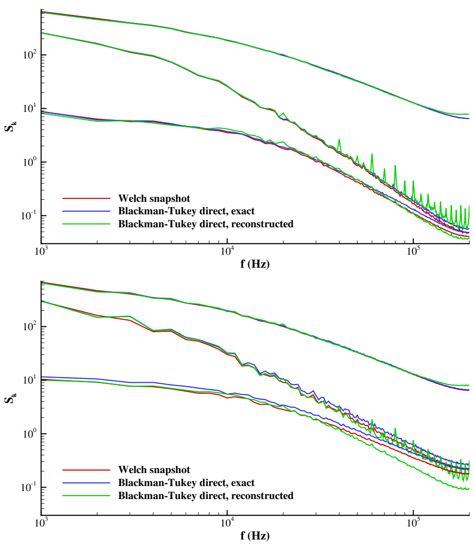

Figure 4. Turbulent kinetic energy spectra for the sum of all modes, for modes 1 and for modes 10, obtained from the LES database using all the time samples (top) or using only one-seventh of them (bottom).

Application to the dual-PIV database

The Blackman-Tukey Direct SPOD algorithm with reconstruction of cross-correlations has been applied to the dual-PIV measurements and to the LES database, from which 560 samples, de-correlated as much as possible, have been extracted over the same 70×16 grid as in the previous section. To this end, velocity snapshots were randomly sampled in time across the full duration of the database and four distinct streamwise–wall-normal planes distributed along the span, with an average sampling interval equal to 160 ± 65 of the original sampling time. The number of samples extracted from the LES corresponds to the mean values of the PIV image pairs available for a given time delay τ_i. For the sake of comparison, the Welch snapshot algorithm was also used with a continuous time series of 4000 consecutive, highly correlated, samples, split into 19 segments with 50% overlap. These values ensure a similar frequency resolution and statistical uncertainty as achieved with the random sampling of 560 mostly de-correlated samples used for the Blackman-Tukey algorithm.

The turbulent kinetic energy spectra obtained from the three SPODs are plotted in Fig. 6. The Blackman-Tukey spec-

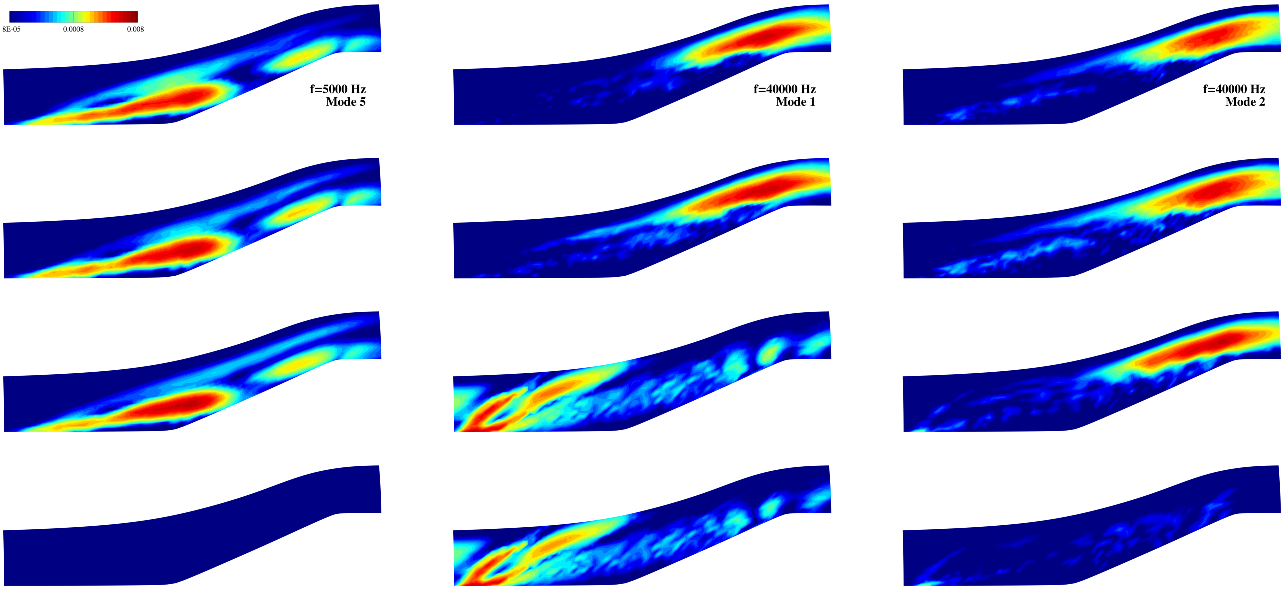

Figure 5. Map of normalized turbulent kinetic energy for mode 5 at f=5000 Hz (left), mode 1 at f=40000 Hz (middle) and mode 2 at f=40000 Hz (right). From top to bottom: Welch snapshot method, Blackman-Tukey direct method with exact cross-correlations, Blackman-Tukey direct method with reconstructed cross-correlations and difference between the Blackman-Tukey direct method with exact and reconstructed cross-correlations.

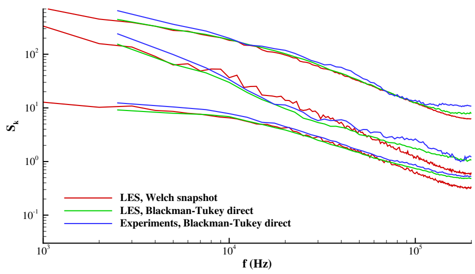

Figure 6. Turbulent kinetic energy spectra for the sum of all modes, modes 1 and mode 10.

tra obtained from the experiments and the LES match very well. Main differences are a larger energy content at low frequencies for the experiment, confirming Larchevêque *et al.* (2023), as well as a slightly increased range of aliasing in the case of the dual-PIV database, which is associated with a slightly lower space resolution of the measurements. Compared with the Welch snapshot spectra, the Blackman-Tukey Direct spectra show an increased level of turbulent kinetic energy in the modes above 70 kHz. The origin of this difference remains to be investigated but does not appear to be related to statistical uncertainty, since the Blackman-Tukey spectra obtained using 4000 consecutive samples rather than the 560 random samples (not shown) exhibit opposite trends, in line with what was observed in the lower plot of Fig. 4.

The turbulent kinetic energy space maps of the first four modes at $f = 5000\,\mathrm{Hz}$ are plotted in Fig. 7. The differences between the modes obtained from Blackman-Tukey applied to the dual-PIV and the LES data are reminiscent of the differences found for the standard POD modes in Larchevêque *et al.* (2023). Modes 1 and modes 2 (LES)-3(experiments) have similar structures, whereas higher-order modes appear to have mixed / shared features between the LES (3 and 4) and the dual-PIV (2 and 4) modes. The Welch-snapshot-SPOD modes exhibit less defined structures for high-order modes, presumably due to a lack of convergence related to the modulation of this frequency range by the lower frequencies that are associated with the breathing of the separated region. In fact, the 4000 continuously sampled snapshots encompass about 4 low-frequency cycles, whereas the random sampling used with the Blackman-Tukey method extracts data over 90 cycles.

For higher frequencies up to about 25 kHz, it is possible to find a reliable correspondence between the first two or three modes from LES and experiment, although sometimes with a different rank due to the narrower energy difference between modes with increasing frequency. This behavior is illustrated in Fig. 8 for a frequency of 20 kHz, with LES modes 1 and 2 reasonably matching modes 3 and 1 obtained from dual-PIV.

For higher frequencies, the energy gap between modes is much reduced, as visible in Fig. 6, and the 2-point coherence tends towards 0 (see Fig.3). Combined with the large statistical uncertainty due to the limited number of samples, this makes the extraction of coherent behavior through SPOD mostly irrelevant beyond the first SPOD modes, as they roughly correspond to the spatial Fourier transform of white noise.

CONCLUSIONS AND FUTURE WORK

The reconstruction method of Jiang *et al.* (2017) has been extended to two–point and two–component cross-spectral densities of all three velocity components obtained from dual–PIV measurements. Analyses based on a synthetic database obtained from a LES computation of a M=2.52 shock-wave – turbulent-boundary layer interaction, reproducing the sampling characteristics of the dual-PIV system, demonstrated the accuracy of the method regardless of the locations of the sensors throughout the flow field and of the velocity components under consideration.

This accuracy makes it possible to compute a Spectral Proper Orthogonal Decomposition using an original approach based on the Blackman-Tukey method. Using the LES dataset, we demonstrate that this algorithm yields results similar to those of an SPOD based on the classical Welch snapshot approach.

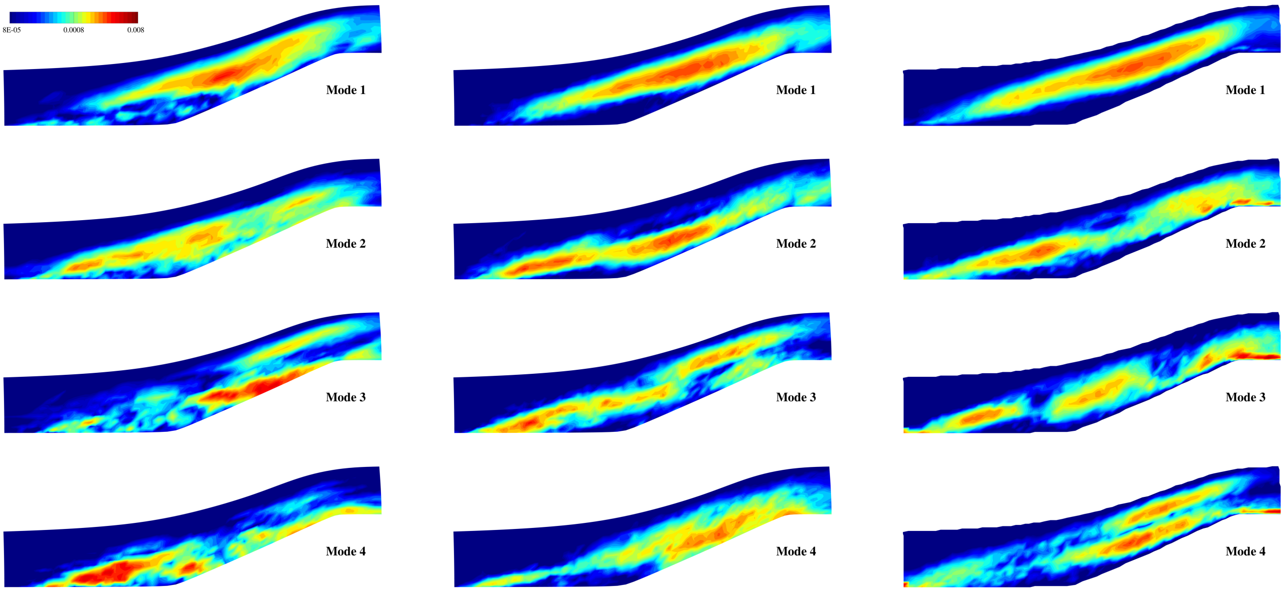

Figure 7. Map of normalized turbulent kinetic energy for modes 1 to 4 at f=5000 Hz from the Welch snapshot method applied to the shortened LES database (left) and from the Blackman-Tukey method with reconstructed cross-correlations, either from random samplings of the LES database (center) or from the dual-PIV measurements (right).

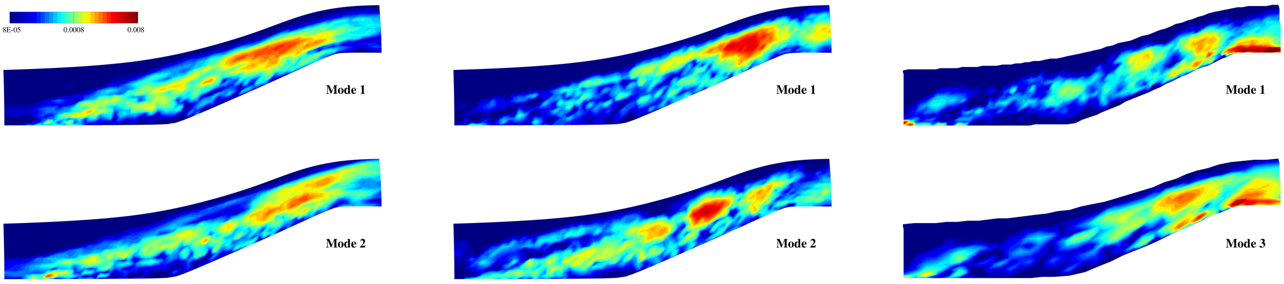

Figure 8. Map of normalized turbulent kinetic energy for selected modes at f=20000 Hz. See the caption of Fig. 7 for a description of the columnar arrangement of the plots.

The algorithm was then applied jointly to the experimental database and a subset of the LES database emulating the sampling characteristics of the PIV data. This approach allowed us to extend the detailed analysis of similarities and differences between the experimental and simulated data initiated in Larchevêque *et al.* (2023). Beyond the specific flow studied here, the suggested method appears to be of interest for the detailed analysis of coherent structures developing in high-speed transitional and turbulent flows.

Future work will include the computation of an SPOD of the present flow with a number of points that are one order of magnitude larger than the calculations presented in this paper, as well as attempts to regularise cross-spectral density estimates by taking advantage of the presence of spurious negative eigenvalues in the cross-spectral matrix.

REFERENCES

Jiang, T., Schreyer, A.-M., Larchevêque, L., Piponniau, S. & Dupont, P. 2017 Velocity Spectrum Estimation in Shock-Wave/Turbulent Boundary-Layer Interaction. *AIAA Journal* **55** (10), 3486–3498.

Larchevêque, L., Ramaswamy, D.P. & Schreyer, A.-M. 2023 Effects of favourable downstream pressure gradients on separated shock-wave/boundary-layer interactions. *International Journal of Heat and Fluid Flow* **102**, 109164.

Lumley, J. L. 1967 *The structure of inhomogeneous turbulent flows*, p. 221–227. Moscow: Nauka.

Ramaswamy, D.P., Schauerte, C.J. & Schreyer, A.-M. 2023 A New Dual-Stereo-PIV System for Spatio-Temporal Measurements of 3D Unsteady Flows. In *Proceedings of the 15th International Symposium on Particle Image Velocimetry (ISPIV 2023)*. San Diego, USA.

Schmidt, O.T. & Colonius, T. 2020 Guide to Spectral Proper Orthogonal Decomposition. *AIAA Journal* **58** (3), 1023–1033.

Schreyer, A.-M., Larchevêque, L. & Dupont, P. 2016 Method for spectra estimation from high-speed experimental data. *AIAA Journal* **54** (2), 557–568.

Schreyer, A.-M., Lasserre, J.J. & Dupont, P. 2015 Development of a dual-piv system for high-speed flow applications. *Experiments in Fluids* **56**, 187.

Sirovich, L. 1987 Turbulence and the dynamics of coherent structures part I : Coherent structures. *Quart. Appl. Math.* **45** (3), 561–571.

Stineman, R. W. 1980 A consistently well-behaved method of interpolation. *Creative Computing* **6** (7), 54–57.